Civil Engineering Dimension
https://ced.petra.ac.id

Seismic Performance of Base-Isolated Buildings with Vertically Staggered Foundations on Hilly Terrain under Near- and Far-Field Earthquakes

Barik, J.R.[1]*, Parashar, A.[2], and Biswal, K.C.[2]
[1] Department of Ocean Engineering, Indian Institute of Technology Madras, Tamil Nadu, INDIA
[2] Department of Civil Engineering, National Institute of Technology Rourkela, Odisha, INDIA

DOI: https://doi.org/10.9744/ced.28.2.291-308

Article Info:
Submitted: Apr 06, 2026
Reviewed: May 06, 2026
Accepted: July 21, 2026

Keywords:
staggered foundation,
irregular building,
near-field and far-field earthquakes,
lead rubber bearing.

Corresponding Author:
Barik, J.R.
Department of Ocean Engineering,
Indian Institute of Technology Madras,
Tamil Nadu, INDIA
Email: jyotiranjanbarik0@gmail.com

Abstract

Rapid urbanization and limited land availability have encouraged construction on sloping terrains, where framed structures remain highly vulnerable to seismic damage. Base isolation provides a proven means of enhancing resilience. This study investigates staggered buildings equipped with isolation systems, specifically lead rubber bearings, under near-field and far-field earthquakes using ETABS models of isolated and non-isolated irregular structures. Results for regular buildings were validated against existing solutions. Slope angles between 0° and 45° were analyzed to assess seismic parameters including vibration period, base shear, storey displacement, drift, and overturning moment. Findings show that near-field earthquakes intensify slope effects, amplifying base shear, displacement, drift, and overturning moment, while far-field motions exhibit lower sensitivity. Base isolation consistently reduced force-based responses across slope angles, though displacement amplification was most pronounced in steep-slope buildings under near-field motions. Overall, base isolation demonstrates strong potential to improve seismic safety and resilience of staggered buildings in hilly terrains.

INTRODUCTION

Rapid urbanization and economic expansion have significantly increased the population densities in hilly regions, leading to a higher demand for multi-storey buildings such as reinforced concrete framed hospitals, colleges, hotels, and offices resting on hilly slopes [1,2]. However, the lack of availability of level land in some regions necessitates the construction of buildings on steep slopes. When subjected to seismic forces, buildings built on hill slopes behave differently than those built on level ground. While constructing building structures on steep slopes, a step-back (or staggered) configuration is the most optimal choice [3,4]. Since the seismic behavior of buildings is governed by the distribution of mass and stiffness in both the horizontal and vertical planes, the irregularity and asymmetry introduced by step-back configurations in hilly buildings lead to non-uniform distributions of mass and stiffness, resulting in complex seismic responses. Consequently, such asymmetrical structural configuration creates irregular variations in stiffness and mass across different floors. During an external seismic force, such variations develop torsional moments as well as uneven lateral forces [5-7]. One of the challenges with step-back buildings is that the shorter columns on the uphill side attract higher lateral forces, which can lead to the failure of these columns. The stiffness and strength characteristics of the walls play a crucial role in determining the lateral load capacity shared by the structure [2,8,9].

Note : Discussion is expected before November, 1st 2026, and will be published in the "Civil Engineering Dimension", volume 29, number 1, March 2027.
ISSN : 1410-9530 print / 1979-570X online
Published by : **Petra Christian University**

Earthquake impact has amplified the problem of landslide and erosion in the hilly regions thus all buildings in the hilly regions must be analyzed for the seismic loads. Previous studies of earthquakes in hill regions demonstrate that buildings with varied heights of columns within the same level were the most sensitive to earthquake damage. Therefore, the buildings must be designed to obtain adequate resistance to prevent the loss of life and property. Numerous studies have focused on buildings in hilly terrains in recent years [10-18]. However, the studies have witnessed various challenges and proposed different techniques for mathematical modelling and seismic analysis of staggered base non-isolated buildings. The studies conducted so far have given the idea about the structural behavior of hill buildings but their performance in different configurations has not been assessed scrupulously. Research projects have been conducted around the world in recent decades to examine the causes of the failure of various types of buildings during strong seismic excitations, while also investigating innovative seismic protection and strengthening techniques, including buckling restrained braces for irregular reinforced concrete buildings and elastomeric bearing links for mitigating seismic pounding between adjacent structures [19-22]. Geological features are found to be very significant in some areas due to the increased demand for space, certain buildings must now be built without altering the existing geological profile. The seismic waves that arrive at an area on the earth's surface are the consequence of complicated superposition, which causes unstable motion and ground shaking [23].

Previous research indicates that the most effective way to control seismic disruption in structural systems is a base isolation system [24-29]. In general, the structural strength is enhanced in conventional earthquake-resistant RC constructions to satisfy the seismic demand by employing appropriate reinforcement and ductility. However, a base isolation system modifies the building's dynamic properties to reduce the shear demand for which the structure is intended. Thus, by creating a flexible intermediate system between the foundation and the base of the columns, the damping and horizontal flexibility of a building can be suitably improved. Furthermore, a significant dynamic amplification effect arises from the fact that reinforced concrete structures frequently occur within the range of the dominant period of seismic excitations [30]. In order to reduce the seismic demand greatly, the vibration period of the building can be increased beyond a specified limit by implementing foundation isolation [31-33]. Among the passive bearing isolation strategies, the lead core isolator is the most popular type of isolator due to its proven effectiveness in reducing the effects of high-frequency vibrations and greater accelerations [34-38]. In addition, such an isolator's stiffness is higher in the vertical direction and lower in the horizontal direction.

Recent seismic events have highlighted the need to ensure the safety and reliability of Reinforced Concrete Moment Resisting Frame (RC-MRF) buildings, emphasizing the importance of accurate modelling approaches in predicting seismic demands and structural responses [39-41]. With the evolution of modern isolation technology, Ma et al. [42] investigated the seismic performance of base-isolated and story-adding isolated structures, emphasizing their dynamic response under near-fault and far-fault ground motions. Recent developments in staggered storey isolated structures have focused on enhancing isolation performance and addressing challenges posed by long-duration and complex seismic events [43-45]. Shu et al. [46] developed a revolutionary staggered storey isolated structure, evaluating its seismic performance through numerical simulations, varying isolation layer positions and chassis areas, and demonstrating effective isolation and reduced structural damage under ground motion.

Extensive research exists on the seismic performance of base-isolated buildings on flat terrain [47–52], but studies focusing on base-isolated reinforced concrete structures on hilly terrains with staggered foundations remain limited. Moreover, the influence of earthquake source characteristics on the seismic response of such structures has not been adequately explored. Near-field and far-field ground motions can impose significantly different seismic demands, particularly on flexible base-isolated systems. Near-field earthquakes are often associated with pulse-like motions that can amplify displacement, drift, and overturning responses, whereas far-field earthquakes generally exhibit more distributed frequency content, resulting in different structural response patterns [53-54]. Most prior work has dealt with conventional fixed-base step-back or step-back–setback configurations, neglecting base isolation as well as the dynamic response of vertically irregular, staggered buildings, especially when subjected to near-field and far-field earthquakes. In particular, the influence of widely adopted lead rubber bearings (LRBs) on critical seismic response parameters such as fundamental period, base shear, storey displacement, drift, and overturning moment in buildings built on variable slopes has not been systematically investigated.

This study addresses this key gap by conducting a comprehensive evaluation of step-back base-isolated buildings on sloped terrains using LRBs, considering both near-field and far-field earthquake scenarios. Such investigation focuses on near-field and far-field earthquake scenarios, providing critical insights into the effectiveness of base isolation for structures on irregular topography. Models developed in ETABS software incorporate varied slope angles and geometric irregularities, in accordance with IS 1893:2016 guidelines [55–59]. The analysis includes a threedimensional seismic assessment capturing inelastic structural behavior under seismic loading. Important performance metrics such as storey drift and base shear are quantified across multiple slope configurations and six different earthquake records. By systematically evaluating the combined effects of slope angle variation and base isolation, this study provides novel insights and design guidance for safe, sustainable construction in hilly regions, thereby advancing seismic-resistant design and vibration control strategies for complex terrains.

ANALYSIS OF ISOLATED BUILDING WITH STAGGERED FOUNDATION

A building with a staggered base is a structure where the foundation levels are at different levels. Similarly, staggered base isolation is a structural arrangement at which the base isolators are installed at several building levels, as shown in Figure 1. Using ETABS, fixed base and base-isolated buildings at different slope angles ranging from 0^0 to 45^0 are modelled. The buildings are assumed to be constructed on a stiff soil or rock foundation due to which the soil-structure interaction (SSI) effect is neglected. The ETABS modelling approach involves defining geometry, materials, loads, boundary conditions, and performing dynamic analysis using finite elements, ensuring accurate simulation of structural behavior under various earthquakes.

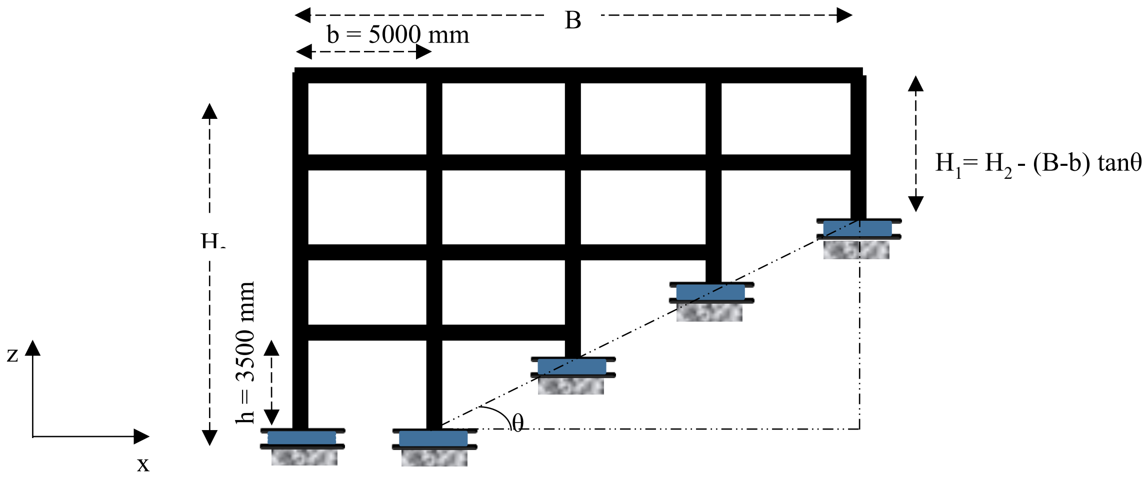

Figure 1. Schematic Elevation of a Base-Isolated Building with Staggered Foundation

Model Validation

A six-storey base-isolated regular building without masonry infill is modelled using lead rubber bearing, as presented by Shirol and Kori [60]. The schematic diagrams of the fixed base and base-isolated buildings are shown in Figure 2. Using ETABS, both equivalent static (ESA) and response spectrum (RSA) analyses are conducted by following the IS 1893:2016 [55-59]. Rigid diaphragm action was assumed at each floor level whereas the properties of building, load considerations, and characteristics of lead rubber bearing are presented in Table 1, 2, and 3 respectively. The seismic loads were applied using the design response spectrum of IS 1893:2016, assuming a damping ratio of 5% for the superstructure and 10% for the isolation system. Rigid diaphragm action was assumed at each floor level, while soil–structure interaction was neglected by considering the foundation as stiff type and the RSA was performed in both horizontal directions. Figures 3 and 4 illustrate the comparison of the vibration period and base shear where the results are in very good agreement with the reported responses.

Table 1. Building Data

Parameter	Value
Typical floor height	3500 mm
Bay width in x-direction	5000 mm
Bay width in y-direction	4000 mm
Size of beams	230 mm × 450 mm
Column size	300 mm × 600 mm
Thickness of slab	150 mm
Wall thickness	230 mm
Grade of concrete	M-30
Grade of steel	Fe-500
Seismic zone	IV (0.24)

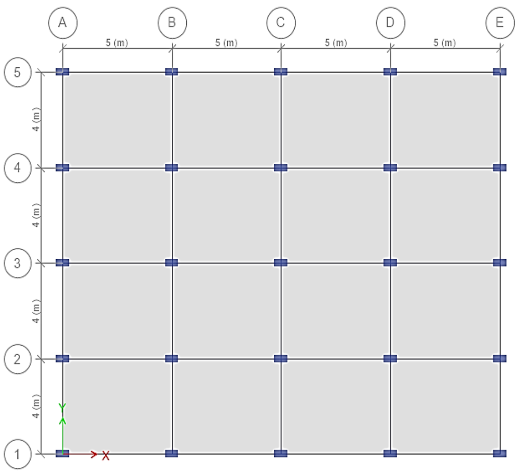

(a) Plan of the Building

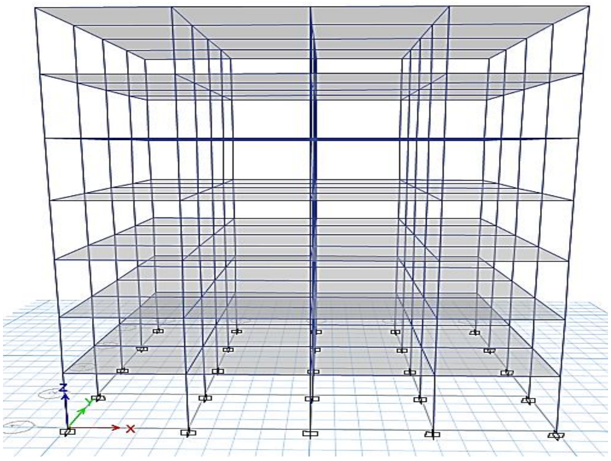

(b) 3D View of Fixed Base Building

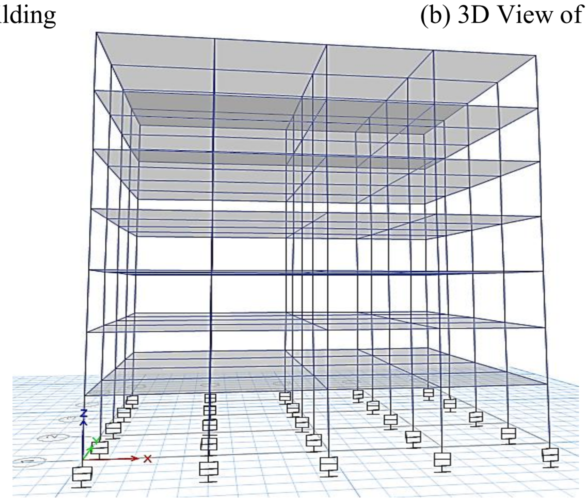

(c) 3D View of Base-Isolated Building

Figure 2. Schematic Diagrams of Buildings for Model Validation (Shirol and Kori [60])

Table 2. Loads Considerations

Loading	Floor	Terrace
Live load	3.0 kN/m²	1.5 kN/m²
Floor finish	1.5 kN/m²	1.5 kN/m²
Wall load	16 kN/m	4 kN/m
Percentage of live load taken	50 % (As per IS: 1893 (Part-I – 2002))	

Table 3. Properties of Lead Rubber Isolator

Property	Value
Effective horizontal stiffness	1416 kN/m
Post yield stiffness	11940 kN/m
Vertical stiffness	530000 kN/m
Short term yield force	46 kN
Post yield stiffness ratio	0.1
Effective damping	0.1

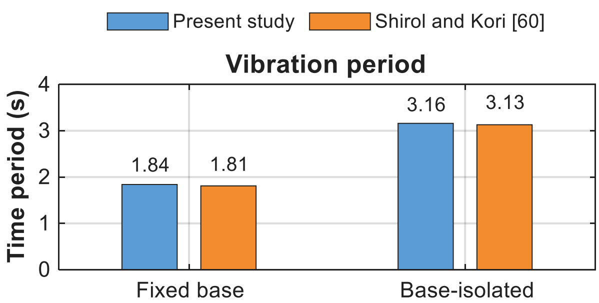

Figure 3. Validation of Vibration Period for Different Buildings

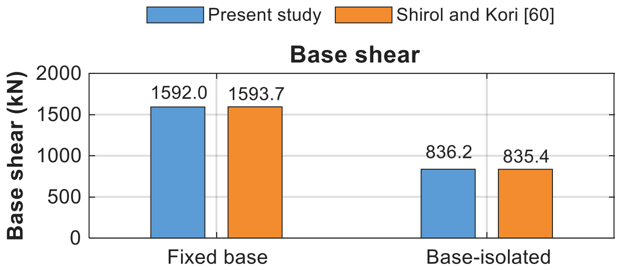

(a) Equivalent Static Analysis

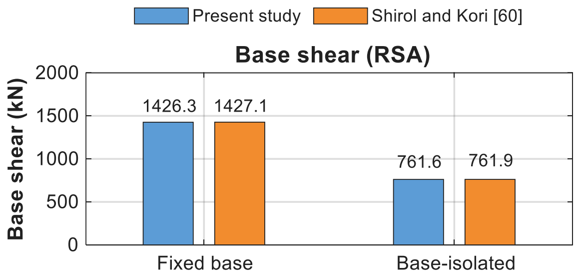

(b) Response Spectrum Analysis

Figure 4. Validation of Base Shear for Different Buildings

Design of LRB

LRBs are the advanced seismic isolation systems utilized to protect structures during earthquakes. During their manufacturing process, a lead plug is added through the rubber laminates. During an external vibration, the lead core deforms plastically, absorbing and dissipating energy through heat generation. Due to this characteristic, the seismic forces transmitted to the structure are substantially minimized. Figure 5 illustrates a schematic diagram of LRB and its hysteresis characteristic.

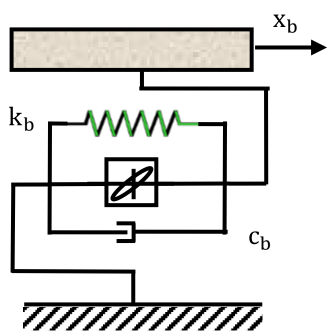

(a) Dash-pot Model

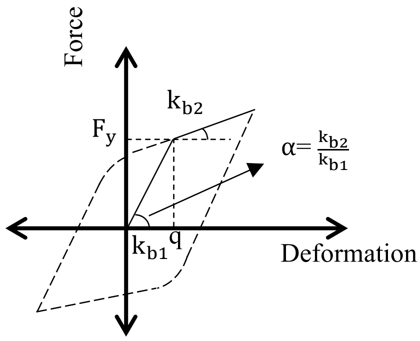

(b) Hysteretic Behavior

Figure 5. Analytical Model of LRB

To analyze and design a base-isolated structure, the properties of LRB need to be evaluated since the properties vary with the dimension of the superstructure. Therefore, a non-isolated building (G+7 storey) is modelled in ETABS as per the specifications listed in Table 4 and the maximum reaction is obtained from the load combinations as per IS 875 (Part 1, Part 2, and Part 5). Subsequently, LRB is designed for this maximum reaction in addition to a targeted period. From the investigation, the isolation characteristics are provided in Table 5. The detailed design is provided in the appendix.

Table 4. Building Parameters

Parameter	Value
No. of stories	G+7
Height of each storey	3.5 m
No. of bays in X direction	4 at 5 m spacing
No. of bays in Y direction	4 at 4 m spacing
Beam size	0.4 m × 0.5 m
Column Size	0.5 m × 0.5 m
Slab thickness	0.15 m
Grade of concrete	M30
Grade for longitudinal reinforcement	Fe500
Grade for transverse reinforcement	Fe415
Beam reinforcement details	4 nos. of 16 mm diameter
Beam stirrup details	10 mm diameter @ 150 mm c/c
Column reinforcement details	8 nos. of 20 mm diameter
Column ties details	10 mm diameter @ 200 mm c/c

Table 5. Properties of Lead Rubber Bearing

Property	Value
Effective horizontal stiffness	1036 kN/m
Axial vertical stiffness	961872 kN/m
Short term yield force (F_y)	240 kN
Effective damping	0.1
Post to pre-yield stiffness ratio (α)	0.1
Pre-yield stiffness (k_{b1})	2400 kN/m
Post-yield stiffness (k_{b2})	240 kN/m
Diameter of the lead core	0.166 m
Diameter of the isolator	0.664 m
Modulus of rigidity	1 MPa
Bulk modulus	2000 MPa
Yield displacement of the bearing (q)	0.125 m

Design of Building

Non-isolated and base-isolated buildings at different slope angles 0°, 15°, 30° and 45° are modelled using ETABS. The structural members were modelled considering elastic behavior to simplify the analysis and focus on the comparative influence of slope and isolation. The geometry considered in this study, i.e., a G+7 storey reinforced concrete moment-resisting frame with staggered foundations, reflects common construction practices in hilly regions where step-back configurations are widely adopted due to terrain constraints. In particular, this type of configuration corresponds to the vertical geometric irregularity illustrated in IS 1893 (Part 1), which highlights irregularity due to unequal floor levels. Lead Rubber Bearings (LRBs) were selected as the isolation system because of their proven effectiveness in Indian seismic applications and their codal support under IS 1893 (Part 6). Loads are considered as per IS 875 Part 1 and Part 2 where the self-weight of beam members is 13.86 kN/m. In addition, live load at the roof level is considered as 1.50 kN/m^{2,} and at each floor level is 3.0 kN/m^2. The side face elevation of the isolated building model prototypes with slope angles of 0^0 and 45^0 is shown in Figure 6.

Earthquake Ground Motion Data

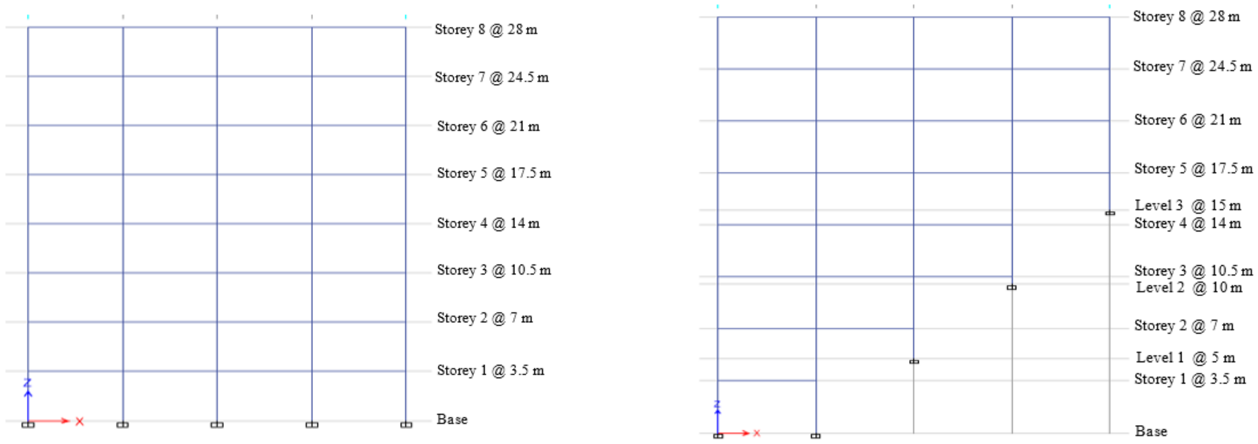

(a) (b)

Figure 6. Side Elevation of Isolated Building Model Prototypes: (a) at 0^0 slope, (b) at 45° slope

A total of six ground motions are selected for the seismic analysis based on the near-field and far-field characteristics. The earthquake data was extracted from the PEER ground motion database and a detailed description is provided in Table 6. Variation in ground motion parameters is taken into consideration by selecting a set of earthquake records that reflect a broad range of seismic characteristics. These include differences in earthquake magnitude, source-to-site distance (R_{rup}), peak ground acceleration (PGA), and fault mechanisms. Additionally, the selected motions originate from different fault types - reverse-oblique and strike-slip—introducing variability in rupture behavior and ground motion characteristics. Site conditions also differ, covering NEHRP Site Classes C and D, which influence ground motion amplification. This comprehensive selection ensures that the variability in frequency content, duration, and amplitude of seismic inputs is adequately represented in the analysis. The time history of earthquakes is illustrated in Figure 7. During the analysis, the peak ground acceleration (PGA) of all the earthquakes is scaled to 0.3g.

Table 6. Description of the Ground Motions

Type of Earthquake	Notation	Earthquakes	Station	Magnitude	R_{rup} (Km)	Soil Type (NEHRP Class)	Fault Mechanism	PGA (g)	PGV (Cm/S)	PGA/PGV (Hz)
Near Field	NF1	Northridge (1994)	Jensen Filter Plant	6.69	5.43	Class D (Stiff Soil)	Reverse (oblique)	0.617	66.1	9.16
	NF2	Imperial valley (1979)	Bonds Corner	6.53	2.66	Class D (Stiff Soil)	Strike-slip	0.777	44.1	17.3
	NF3	Imperial valley (1979)	El Centro Array	6.53	0.07	Class D (Stiff Soil)	Strike-slip	0.317	112.5	2.77
Far Field	FF1	Northridge (1994)	Anaverde Valley - City R	6.69	37.67	Class D (Stiff Soil)	Reverse (oblique)	0.061	5.5	10.9
	FF2	Imperial valley (1979)	Coachella Canal #4	6.53	50.1	Class E (Soft Soil)	Strike-slip	0.128	15.4	8.16
	FF3	Imperial valley (1979)	Plaster City	6.53	30.33	Class E (Soft Soil)	Strike-slip	0.057	4.0	14.0

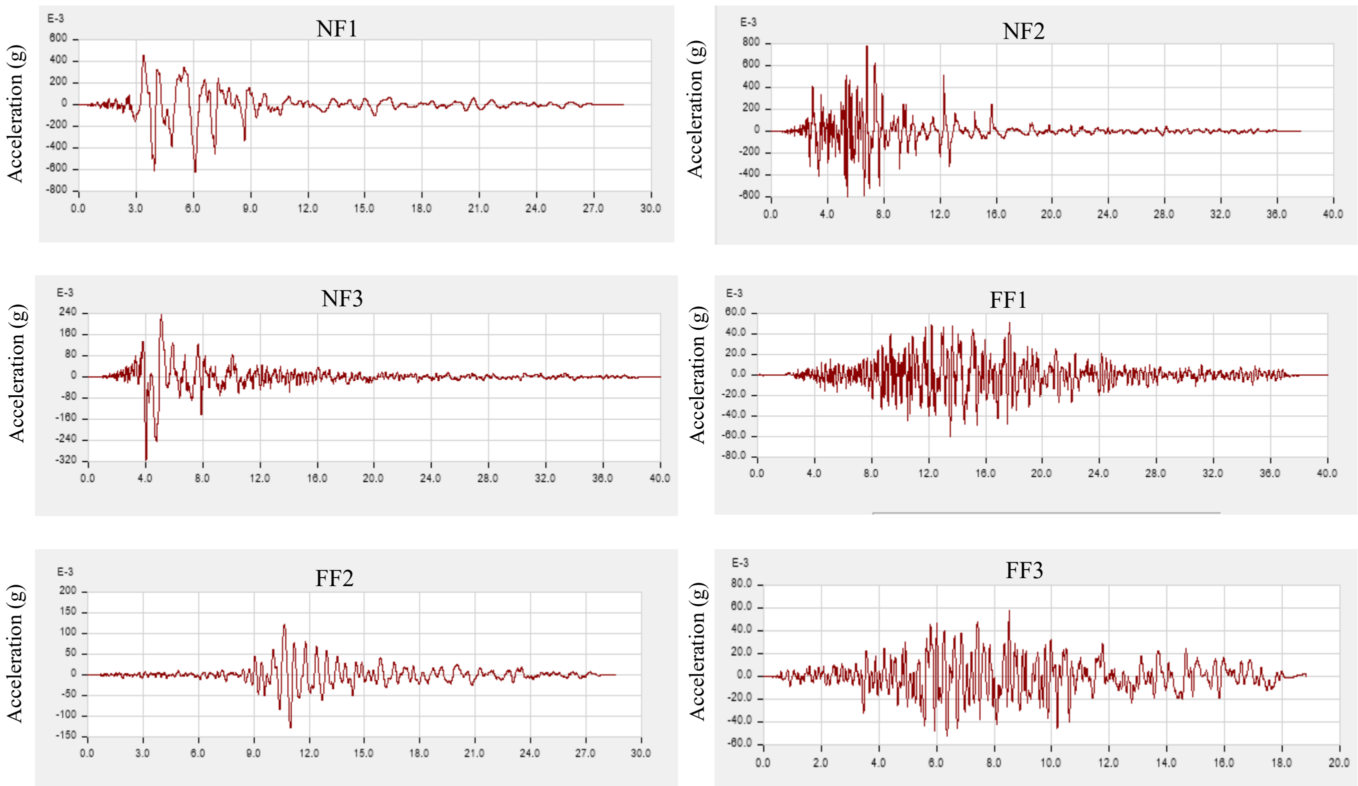

Figure 7. Time History of Ground Motions

RESULTS AND DISCUSSION

The structural models comprised of fixed base buildings and base-isolated buildings are analyzed and compared for each slope angle for response quantities like fundamental period, base shear, maximum inter-storey drift, and overturning under near-field and far-field earthquake ground motions. A detailed description of the behavior of the responses is provided below.

Fundamental Vibration Period and Frequency

The fundamental vibration period plays a critical role in determining a structure's seismic response, as it helps avoid resonance conditions that could amplify forces and cause significant damage. For both fixed-base and base-isolated buildings, the vibration period is measured through a free vibration analysis, with the results summarized in Table 7. The findings show that the vibration period decreases as the slope angle increases, which reflects an increase in structural rigidity. This trend remains consistent, irrespective of the use of base isolation. To better understand the impact of slope angles, the percentage reduction in the vibration period is calculated relative to a structure with a 0° slope. These results, as presented in Figure 8, highlight that slope angles have a more pronounced effect on the vibration period of fixed-base buildings compared to base-isolated ones. While base isolation significantly increases the fundamental vibration period, changes in slope angle have only a minimal impact on this increase. The data emphasize that base isolation effectively extends the vibration period, improving the seismic performance of the structure. However, as slope angles increase, both fixed-base and base-isolated buildings exhibit increased rigidity, reducing their vibration periods proportionally.

Table 7. Fundamental Vibration Period and Frequency of Different Configurations of the Structures

Slope angle (in degrees)	Vibration period (s)		Frequency (Hz)	
	Fixed base	Base-isolated	Fixed base	Base-isolated
0	1.24	2.91	0.81	0.34
15	1.12	2.76	0.89	0.36
30	0.91	2.69	1.09	0.37
45	0.72	2.62	1.39	0.38

In terms of vibration frequency, an inverse trend is observed. As slope angle increases, the natural frequency of fixed-base structures rises from 0.81 Hz at 0° to 1.39 Hz at 45°, indicating increased stiffness and a corresponding reduction in period. For base-isolated buildings, however, the frequency remains nearly constant, varying only slightly between 0.34 Hz and 0.38 Hz across slope angles. This stability demonstrates the dominance of the isolation system in controlling the dynamic characteristics of the structure, making it far less sensitive to geometric irregularities.

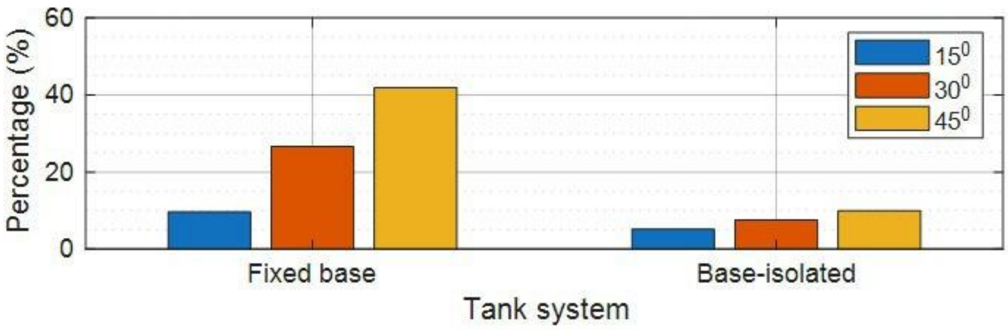

Figure 8. Variation of Fundamental Vibration Period due to the Change in Slope Angle of the Structure

Base Shear Response

Seismic assessment of base shear is also essential during an engineering design practice to ensure that a structure can withstand seismic forces without excessive deformation or collapse. In view of this, the peak base shear values for different configurations of the structures are measured and presented in Table 8. It is observed that fixed-base buildings experience significantly higher base shear forces compared to their base-isolated counterparts across all earthquake records and slope conditions. This highlights the effectiveness of lead rubber bearings (LRBs) in reducing the seismic forces transferred to the superstructure, thereby improving structural safety. An observable trend in the fixed-base buildings is the increase in base shear as the slope angle increases, particularly under near-field earthquake excitations such as NF1, NF2, and NF3. This reflects the augmented seismic demand due to irregular geometry and stiffness variations caused by the slope, which tends to amplify the lateral forces in these structures. Contrarily, the far-field earthquake records generally induce lower base shear values, indicating that the building's response is less severe under these shaking conditions. Although all earthquake records were scaled to the same PGA, differences in frequency content, velocity pulses, and energy distribution continue to influence the structural response. The pulse-like nature of near-field motions has produced greater dynamic amplification, resulting in higher base shear demands than those induced by far-field earthquakes.

Table 8. Peak Base Shear in Different Earthquakes (kN)

Earthquakes	Fixed base				Base-isolated			
	0^0	15^0	30^0	45^0	0^0	15^0	30^0	45^0
NF1	2331	3413	3670	2079.6	1310.5	805.3	797.9	361
NF2	717	849.2	877	1305	342	148.5	143.2	123.3
NF3	2023	1908	2684	2778	1346.8	1306.4	1216.7	857.3
FF1	230.8	168.9	140	175	64.9	59.3	53.9	42.6
FF2	126	127	97	77.5	43	45	44	28
FF3	682	712	867	907	186.5	173.8	161.1	192.8

For base-isolated buildings, the base shear values are considerably reduced at all slope angles and across all earthquake scenarios, confirming that seismic isolation is highly effective in attenuating earthquake-induced forces. The reductions become even more pronounced at steeper slopes (30° and 45°), suggesting that LRBs not only mitigate seismic loads effectively but also help counteract the amplification effects introduced by the stepped and sloped foundations. Thus, base isolation provides a robust strategy to enhance the resilience of buildings constructed on hilly terrain.

To demonstrate the shear responses in a better way, the percentage reductions due to the change in slope angle and base isolation are estimated. Figure 9 illustrates the reduction percentages due to the staggered configuration relative to the building with a slope angle at 0^0. The figure reveals that base-isolated buildings generally show significant reduction percentages under near-field earthquake records, implying that increasing the slope angle, combined with isolation, can have a beneficial effect in reducing seismic demands. In contrast, fixed-base buildings exhibit inconsistent behavior with some cases showing negative reductions, highlighting that higher slopes can sometimes increase seismic forces, especially in the absence of isolation. Moreover, base-isolated structures exhibit a more significant reduction in base shear compared to fixed-base structures, particularly at higher slope angles (45°). Earthquakes like NF2 and NF3 display the highest reductions, especially for base-isolated structures at 45°, where reductions exceed 50%. As opposed to this, NF1 shows a mix of positive and negative reductions, indicating that in some cases, increasing the slope angle may amplify base shear. For fixed-base structures, the reduction percentages are generally lower, suggesting that base isolation plays a crucial role in minimizing seismic forces. Some earthquakes like FF1 and FF2 show relatively consistent reductions across different slope angles, but variations exist for other earthquake cases.

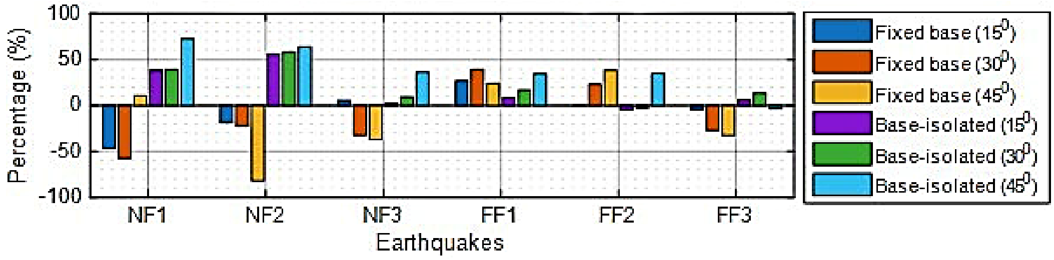

Figure 9. Percentage Reduction in Base Shear due to the Change in Slope Angle

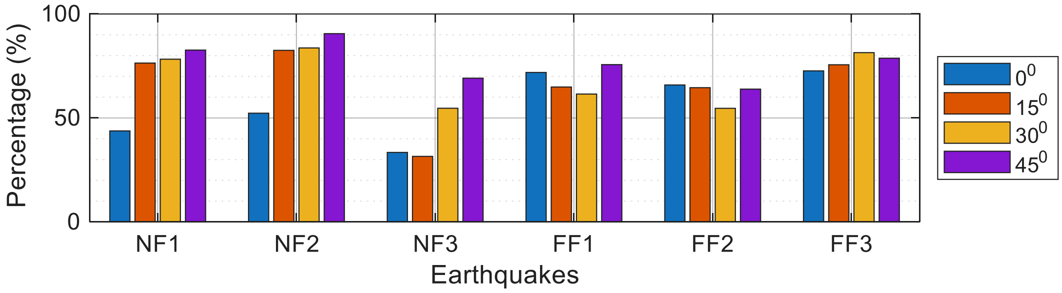

Figure 10. Percentage Reduction in Base Shear due to Base Isolation

Figure 10 compares the effectiveness of base isolation across all slope angles by plotting the percentage reduction in base shear between fixed-base and base-isolated buildings. Results confirm that base isolation consistently leads to substantial reductions, often exceeding 30–50%, across different earthquake types and slope configurations. The most significant benefits are observed when the building rests on a 45° slope, emphasizing the pivotal role of LRBs in mitigating seismic effects for irregular buildings on steep slopes. Overall, the data presented in Table 8 and Figures 9 and 10 collectively underscore the dual influence of slope geometry and base isolation on seismic force demands. While slope increases can elevate base shear in fixed-base buildings, the introduction of LRBs considerably alleviates seismic stresses, making isolation an essential consideration in the design of structures on hilly terrain subjected to both near-field and far-field earthquakes.

Storey Displacement

Assessment of maximum storey displacement has a paramount significance in preventing possible structural failure if the displacement is large under seismic loads. From the analysis, the absolute peak values of the parameter are extracted for both building types subjected to NF1 and FF1 earthquakes, as illustrated in Figure 11. The results consistently show that base-isolated buildings exhibit larger storey displacements when compared to fixed-base counterparts. This behavior is primarily due to the flexible nature of the isolation layer, which allows significant relative movement at the base, effectively decoupling the superstructure from ground motion. In base-isolated structures, the maximum displacement tends to concentrate at the isolation level, i.e., the layer where LRBs are installed. This feature demonstrates the isolators' role in absorbing seismic energy and protecting the superstructure by shifting deformation away from the building frame to the isolation system. Consequently, while the overall displacement increases, the structural components above the isolation system experience much-reduced deformation and damage risk.

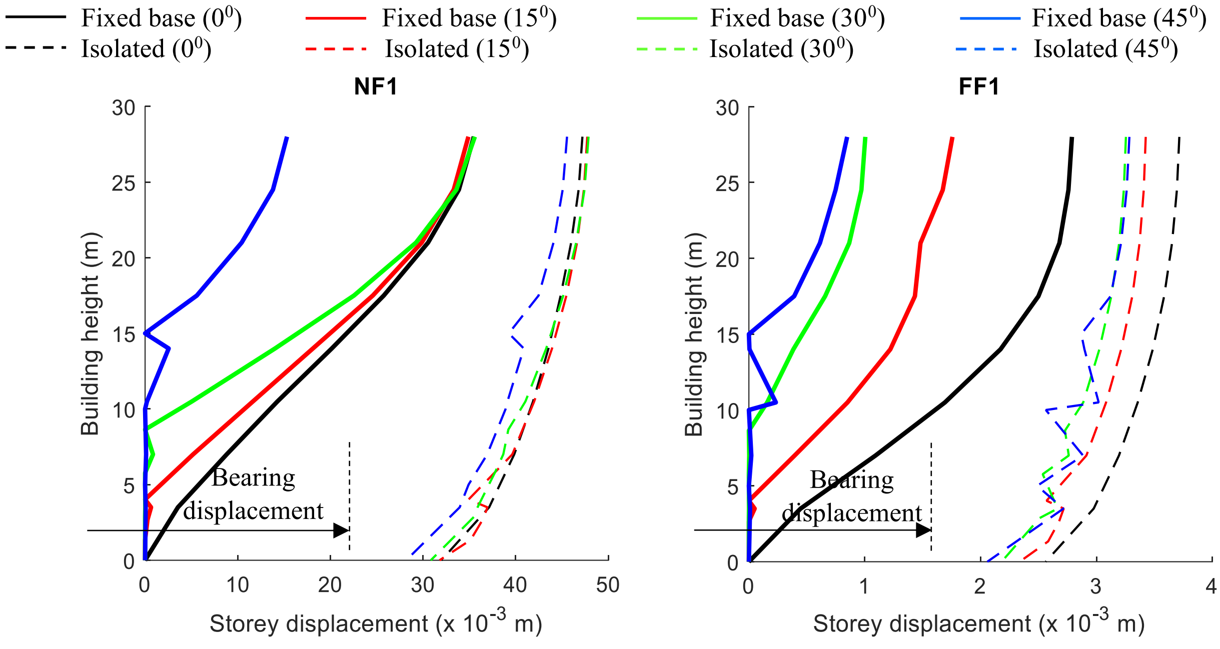

Figure 11. Behavior of Storey Displacement due to the Change in Slope Angle

The effect of increasing slope angle on storey displacement reveals a noticeable trend. For fixed-base buildings, increasing the slope generally results in decreased storey displacement (notably at 45°), likely due to higher stiffness induced by geometric constraints. On the other hand, base-isolated buildings show an increase in storey displacement with slope, particularly pronounced under near-field earthquake excitation such as NF3. This behavior suggests that ground motion characteristics and slope together influence the isolation system's deformation demands, highlighting the complex interactions between site conditions and seismic response.

Table 9. Peak Storey Displacement in Different Earthquakes (mm)

Earthquakes	Fixed base				Base-isolated			
	0^0	15^0	30^0	45^0	0^0	15^0	30^0	45^0
NF1	35.1	45.6	38.1	15.1	47.1	47.3	49.1	40.2
NF2	8.3	8.1	7.7	7.2	9.5	10.1	11.2	13.5
NF3	30.3	25.8	25.7	21.2	81.2	76.2	73.3	66.1
FF1	2.8	2.2	1.4	1.2	4.1	3.5	3.2	3.8
FF2	1.8	1.7	1.2	0.6	2.6	2.6	2.7	2.6
FF3	9.5	9.4	8.3	5.6	12.1	11.2	10.1	11.4

The maximum values are obtained for different staggering cases under all the specified earthquakes, as specified in Table 9. It is evident that the peak displacement is significantly influenced under the near-field characteristics of the earthquakes. In particular, near-field earthquakes, characterized by high-amplitude velocity pulses and concentrated energy over short durations, produce substantially larger displacement demands; therefore, peak story displacements under near-field records are markedly higher than those from far-field events. To examine the behavior under the influence of a staggered base, the percentage reduction is determined, as shown in Figure 12. It has been noticed that the fixed base building at 45^0 slope angle exhibits a higher reduction as compared to others. Furthermore, the storey displacement is increased invariably due to base isolation. Thus, the percentage increase is calculated and presented, as shown in Figure 13. Note that the base-isolated building at 45^0 slope angle exhibits greater amplification as compared to others. While comparing among the earthquakes, the near-field effect of Imperial valley (NF3) possesses a more significant increase, irrespective of the sloped configurations. Overall, it can be inferred that base-isolated buildings demonstrate increased storey displacement concentrated at the isolation level, with amplification effects enhanced by slope steepness and near-field ground motions. This behavior underscores the importance of designing isolation systems capable of accommodating such displacements, especially when constructing on irregular, sloped terrain subjected to diverse seismic hazards.

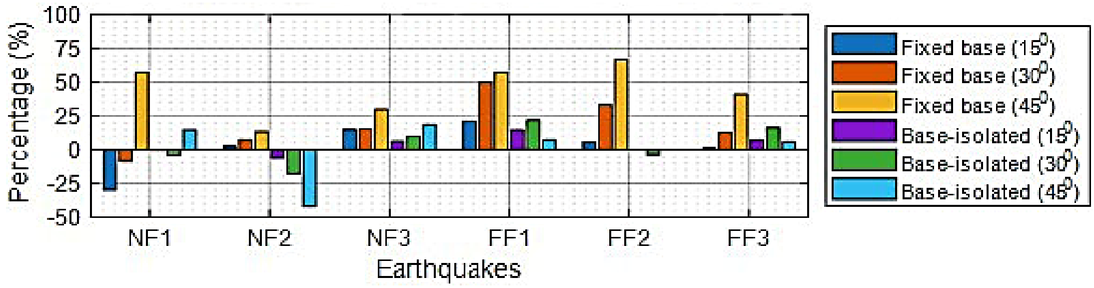

Figure 12. Percentage Reduction in Peak Storey Displacement due to the Change in Slope Angle

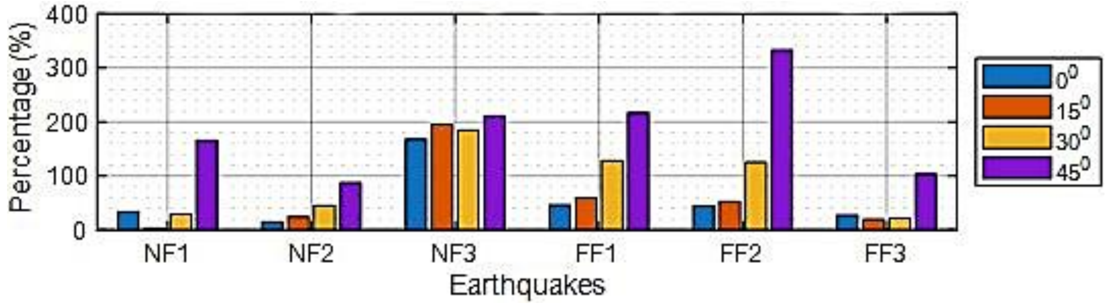

Figure 13. Percentage Increase in Peak Storey Displacement due to Base Isolation

Inter-Storey Drift

The inter-storey drift is an important attribute in a performance-based seismic analysis, which should remain as low as possible to prevent damage to primary structural elements in a structure. With this objective, the inter-storey drift is measured under all the specified ground motions and the peak values are presented in Table 10. For fixed-base buildings, inter-storey drifts tend to increase with slope angle, especially under near-field earthquake records such as NF1, NF2, and NF3. For instance, the NF1 drift increases from 1.88 mm at 0° to 2.16 mm at 45°, indicative of amplified lateral irregularity effects and torsional responses caused by the geometrical asymmetry of the sloped foundation. Conversely, far-field earthquakes generally induce lower drifts, reflecting less intense shaking. In contrast, base-isolated buildings consistently show reduced inter-storey drift values across all slope configurations and earthquake types. The mitigating effect of LRBs is pronounced, with reductions often cutting drifts by half or more. However, drift values in base-isolated structures remain relatively stable across different slope angles, highlighting the effectiveness of isolation in controlling deformation irrespective of foundation slope irregularities.

Table 10. Peak Inter-Storey Drift in Different Earthquakes (mm)

Earthquakes	Fixed base				Base-isolated			
	0^0	15^0	30^0	45^0	0^0	15^0	30^0	45^0
NF1	1.88	1.96	2.08	2.16	1.82	1.80	1.78	1.74
NF2	0.54	0.63	0.74	1.32	0.31	0.29	0.28	0.27
NF3	1.13	1.24	1.64	2.47	3.08	2.86	2.71	2.53
FF1	0.19	0.13	0.13	0.15	0.14	0.13	0.12	0.13
FF2	0.08	0.07	0.06	0.08	0.04	0.04	0.04	0.06
FF3	0.45	0.46	0.43	0.45	0.42	0.39	0.37	0.36

Figures 14 and 15 provide visual insights into these tendencies by portraying the percentage reduction of peak inter-storey drift due to changes in slope angle (Figure 14) and base isolation (Figure 15). Figure 14 illustrates that increasing the slope angle does not guarantee a consistent reduction in drift. Indeed, several cases show negative reduction percentages (implying drift amplification), especially in fixed-base buildings for earthquakes like NF3 and FF1. This uncertainty arises from the complex interplay between the building's irregular geometry and seismic wave characteristics, particularly in near-field scenarios where pulse-like ground motions can amplify lateral responses.

Base-isolated buildings exhibit more consistent and generally positive reductions, suggesting improved performance stability despite slope changes. The influence of earthquake characteristics is evident, as different earthquakes produce varying drift responses. Some earthquakes, such as NF3 for fixed-base structures, exhibit sharp reductions at 30°, while others, like FF1 and FF3 for base-isolated structures, show only minor fluctuations. Overall, the results suggest that base isolation helps moderate drift variations, but slope angle effects remain unpredictable. This highlights the need for detailed structural analysis when designing buildings on sloped terrains, ensuring optimal seismic performance based on site-specific conditions.

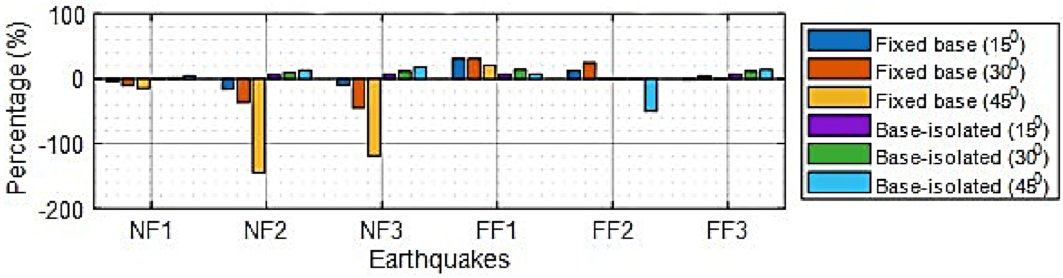

Figure 14. Percentage Reduction in Peak Storey Drift due to the Change in Slope Angle

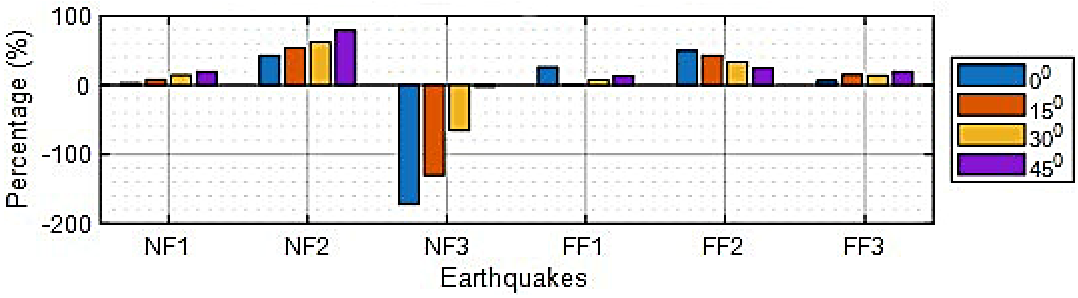

Figure 15. Percentage Reduction in Peak Storey Drift due to Base Isolation

The bar chart in Figure 15 illustrates the reduction in peak story drift due to isolation for various earthquakes. In most cases, isolation effectively reduces peak story drift, with some variations depending on the slope angle. Some earthquakes like NF2 and FF1 exhibit the highest reduction percentages, particularly at higher slope angles (30° and 45°). However, NF3 earthquake shows significant negative reductions at lower slope angles, suggesting that isolation may not always be beneficial in certain conditions. Overall, as the slope angle increases, the reduction in drift remains relatively stable for most earthquake cases, indicating that base isolation performs consistently across different slopes. However, variations in reduction percentages highlight the need for careful design considerations in sloped terrain. Overall, it can be demonstrated that while slope angles can unpredictably influence inter-storey drift, sometimes amplifying this response in fixed-base buildings, the application of lead rubber bearing base isolation generally stabilizes and reduces drift demands across different earthquakes and slope conditions. This underscores the critical role of base isolation in seismic protection strategies for staggered buildings on hilly terrains.

Overturning Moment

Estimation of the overturning moment has a significant role in assessing the rotational stability against the seismic forces. Therefore, the peak values are obtained, as shown in Table 11 for different staggered configurations of the non-isolated and base-isolated buildings. The data clearly show that fixed-base buildings experience significantly higher overturning moments than base-isolated ones across all slope angles and earthquake types. For instance, under the near-field NF1 earthquake, the fixed-base building exhibits a reduction trend while approaching from 0^0 to 45^0, whereas the base-isolated counterpart shows much lower values over the same slope range. This trend indicates that increasing slope angles generally reduce overturning moments, suggesting that the stepped geometry may enhance structural stiffness or alter load distribution favorably.

Figures 16 and 17 provide further insight by illustrating the percentage reduction in peak overturning moments due to slope changes and base isolation, respectively. Figure 16 demonstrates that increasing the slope angle leads to consistent reductions in overturning moments, especially for fixed-base buildings, with reductions reaching up to approximately 75%. This highlights the stiffness and geometric effects introduced by the slope, which can mitigate rotational demands despite the potentially destabilizing irregularity. However, for base-isolated buildings, the slope effect on overturning moment is less prominent, illustrating the overriding influence of the isolation system in controlling seismic response. Figure 17 confirms the substantial benefits of base isolation, showing reductions in overturning moments often nearing or exceeding 90% across various earthquakes and slopes. While the isolation system performs effectively across all slopes, slight reductions in effectiveness occur under certain near-fault excitations (e.g., NF3), reflecting the challenges pulse-like near-field motions pose for isolation systems.

Table 11. Peak Overturning Moment in Different Earthquakes (kNm)

Earthquakes	Fixed base				Base-isolated			
	0^0	15^0	30^0	45^0	0^0	15^0	30^0	45^0
NF1	42699	41623	37583	9863	8892	6336	6089	1930
NF2	11512	10000	10290	7519	2856	2110	1581	1267
NF3	36249	23664	25210	15774	10821	8745	7614	5218
FF1	3341	1516	1189	1186	603	405	349	275
FF2	2143	1740	1257	417	753	497	367	153
FF3	10550	9880	10178	4471	1414	1219	990	689

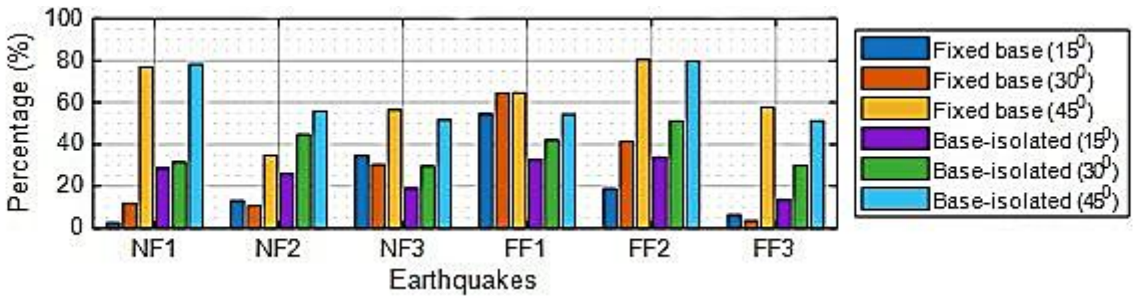

Figure 16. Percentage Reduction in Peak Overturning Moment due to the Change in Slope Angle

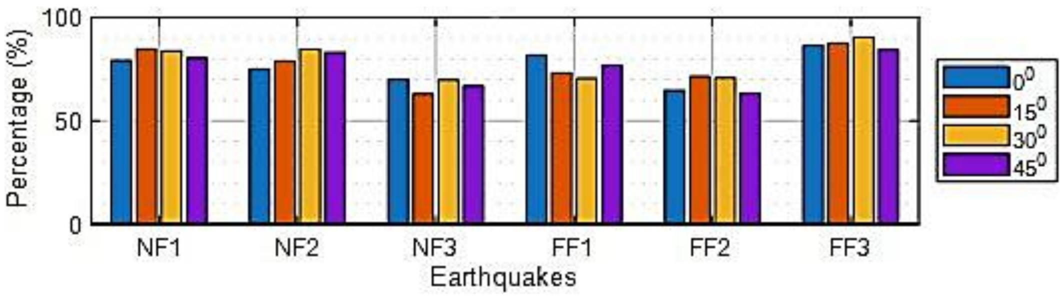

Figure 17. Percentage Reduction in Peak Overturning Moment due to Base Isolation

Overall, base isolation significantly reduces overturning moment response for staggered buildings on hilly terrain, with reductions largely independent of slope angle. This comprehensive discussion integrates quantitative data from Table 11 and analysis of Figure 17, offering critical insights into mitigating seismic overturning moments in irregular, base-isolated structures. Critically, these findings underscore the ability of LRBs to significantly reduce overturning moments, thus enhancing the rotational stability of staggered buildings on complex terrains. Furthermore, the observed decrease in overturning moment with increasing slope angle may be attributed to the increased structural stiffness and altered stiffness distribution associated with steeper staggered configurations, which reduce the seismic overturning demands in the numerical models.

CONCLUSIONS

The influence of both LRB and staggered shape with different slope angles is examined for an eight-storey building under six different near-field and far-field earthquakes using ETABS software. Critical seismic responses such as peak base shear, maximum storey displacement, inter-storey drift, and maximum overturning moment are being assessed. From the investigation, the following conclusions are drawn:

1. The application of LRBs significantly increases the fundamental vibration period of staggered buildings on slopes, effectively shifting their response away from damaging seismic frequencies regardless of slope angle.
2. Increasing slope angle reduces the fundamental period by increasing structural rigidity, but this effect is minimal in base-isolated buildings due to the dominance of the isolation system in controlling dynamic behavior.

3. Base isolation notably reduces seismic demands, such as base shear and overturning moment, under both near-field and far-field earthquakes. Despite the stronger demands imposed by near-field motions, substantial response reductions are achieved across all slope angles, demonstrating the effectiveness of LRBs in enhancing the seismic performance of staggered buildings.
4. For the models considered in this study, base isolation resulted in increased storey displacements concentrated at the isolation layer, with the amplification becoming more pronounced for steeper slopes and under near-field ground motions.
5. While base isolation generally decreases inter-storey drift, slope-induced variability and certain near-fault ground motions can diminish isolation effectiveness, highlighting the need for case-specific seismic assessments.
6. Isolation achieves consistent and substantial reductions (often >50%) in overturning moments across all slope angles, which shows a significant enhancement in the rotational stability of staggered buildings irrespective of the fault-specific earthquakes.
7. The impact of slope angle on key seismic parameters such as period, base shear, drift, and overturning moment, is notably less pronounced in isolated buildings, underscoring the isolator's role in stabilizing response.

This study presents a novel exploration of the combined effects of LRB and slope angles on seismic performance, revealing optimized staggered configurations for enhanced resilience under near-field and far-field earthquakes. The comprehensive numerical evaluation provides essential data for developing design strategies and codes specific to isolated buildings with staggered foundations on sloped terrains. Future research on the seismic analysis of base-isolated buildings with vertically staggered foundations could focus on the following areas:

1. Other innovative isolation techniques can be employed to explore the performance under near-field and far-field earthquakes.
2. The effects of varying soil properties could be investigated on the seismic response of staggered foundations considering soil-structure interaction.
3. The development of design codes and guidelines could be established for specific vertically staggered isolated structures for broader application.

COMPLIANCE WITH ETHICAL STANDARDS

Conflict of interest: The authors state that there is no conflict of interest.

REFERENCES

1. Kumar, S. and Bansal, V.K., A GIS-based Methodology for Safe Site Selection of a Building in a Hilly Region, *Frontiers of Architectural Research*, 5(1), 2016, pp. 39-51.
2. Roshan, P. and Pal, S., Structural Challenges for Seismic Stability of Buildings in Hilly Areas, *Environmental Science and Pollution Research*, 30(44), 2023, pp. 99100-99126.
3. Rc, B., Rani, V., Suleiman, M.F., Biradar, B.B., Vyas, R., Ahmad, A., and Shirkol, A.I., Seismic Performance Evaluation and Comparative Study of Reinforced Concrete Building on a Sloped Terrain with Regular Building by Considering the Effect of URM Infill Walls, *Buildings*, 14(1), 2023, Article 33.
4. Sudeep, Y.H., Ujwal, M.S., Sridhar, H.N., Chandra, S.S., Kumar, G.S., and Ramaraju, H.K., Comparative Study of Step-back and Step-back Setback Configurations of Multi-story Buildings with Varying Height on Sloped Terrain, *Asian Journal of Civil Engineering*, 2024, 25(7), 2024, pp. 5067-5088.
5. De Stefano, M. and Pintucchi, B., A Review of Research on Seismic Behaviour of Irregular Building Structures Since 2002, *Bulletin of Earthquake Engineering*, 6, 2008, pp. 285-308.
6. Gokdemir, H., Ozbasaran, H., Dogan, M., Unluoglu, E., and Albayrak, U., Effects of Torsional Irregularity to Structures During Earthquakes, *Engineering Failure Analysis*, 35, 2013, pp. 713-717.
7. Jain, A. and Surana, M., In-plan Distribution of Peak Floor Acceleration Demands in Torsionally Irregular Buildings, *Journal of Building Engineering*, 90, 2024, Article 109360.
8. Jarapala, R. and Menon, A., Seismic Performance of Reinforced Concrete Buildings on Hill Slopes: A Review, *Journal of the Institution of Engineers (India): Series A*, 104(3), 2023, pp. 721-745.
9. Roshan, P. and Pal, S., Evaluation of Seismic Performance of Hillside Step-back RC Buildings Incorporating Soil-Structure Interaction, *Journal of Vibration Engineering & Technologies*, 13(1), 2025, Article 83.
10. Halkude, S.A., Kalyanshetti, M.G., and Ingle, V.D., Seismic Analysis of Buildings Resting on Sloping Ground with Varying Number of Bays and Hill Slopes, *International Journal of Engineering Research and Technology*, 2(12), 2013, pp. 3632-3640.
11. Surana, M., Singh, Y., and Lang, D.H., Seismic Characterization and Vulnerability of Building Stock in Hilly Regions, *Natural Hazards Review*, 19(1), 2018, Article 04017024.

12. Suresh, G. and Arunakanthi, D.E., Seismic Analysis of Buildings Resting on Sloping Ground and Considering Bracing System, *International Journal of Engineering Research & Technology*, 3, 2014.
13. Aggarwal, Y. and Saha, S.K., Seismic Performance Assessment of Reinforced Concrete Hilly Buildings with Open Story, *Structures*, 34, 2021, pp. 224-238.
14. Jarapala, R. and Biswal, K.C., Dynamic Behavior of Vertically Irregular Sloping Ground Buildings, *Asian Journal of Civil Engineering*, 22(1), 2021, pp. 125-136.
15. Maheshwari, R., Singh, B.K., and Marques, R., Seismic Performance of Confined Versus Unreinforced Masonry Buildings on Hilly Slopes Using Linear Static and Dynamic Analysis Approaches, *Arabian Journal for Science and Engineering*, 48(10), 2023, pp. 13839-13869.
16. Acharya, V. and Sengupta, P., Seismic Vulnerability Assessment of Step-back Hill Buildings Through Experimental Investigation, Numerical Simulation and Fragility Estimation, *Bulletin of Earthquake Engineering*, 22(2), 2024, pp. 395-434.
17. Govindaraju, L., Seismic Behavior of Stepback Buildings with Slope Stability: An Empirical–Numerical Study, *Geotechnical and Geological Engineering*, 42(2), 2024, pp. 1423-1444.
18. Singh, R., Sekhawat, R.S., and Gupta, T., Seismic Response of RCC Buildings on Hill Slopes with Step Back and Step Back-Set Back Configuration, *Journal of Scientific Research and Reports*, 30(3), 2024, pp. 259-274.
19. Warn, G.P. and Ryan, K.L., A Review of Seismic Isolation for Buildings: Historical Development and Research Needs, *Buildings*, 2(3), 2012, pp. 300-325.
20. Gkournelos, P.D., Triantafillou, T.C., and Bournas, D.A., Seismic Upgrading of Existing Reinforced Concrete Buildings: A State-of-the-Art Review, *Engineering Structures*, 240, 2021, Article 112273.
21. Chandra, J., and Warnitchai, P., Application of Buckling Restrained Braces for Seismic Strengthening of Irregular Gravity Load Designed Reinforced Concrete Frame Buildings, *Civil Engineering Dimension*, 13(2), 2011, pp. 65-74.
22. Rahman, M.R.A., Saputra, A., and Satyarno, I., Effectiveness of Elastomeric Bearings in Reducing Pounding Effects between Reinforced Concrete Buildings under Seismic Condition, *Civil Engineering Dimension*, 27(1), 2025, pp. 47-58.
23. Trifunac, M.D., The Role of Strong Motion Rotations in the Response of Structures Near Earthquake Faults, *Soil Dynamics and Earthquake Engineering*, 29(2), 2009, pp. 382-393.
24. Jangid, R.S. and Kelly, J.M., Base Isolation for Near-fault Motions, *Earthquake Engineering & Structural Dynamics*, 30(5), 2001, pp. 691-707.
25. Pan, P., Zamfirescu, D.A.N., Nakashima, M., Nakayasu, N., and Kashiwa, H., Base-isolation Design Practice in Japan: Introduction to the Post-Kobe Approach, *Journal of Earthquake Engineering*, 9(1), 2005, pp. 147-171.
26. Matsagar, V.A. and Jangid, R.S., Base Isolation for Seismic Retrofitting of Structures, *Practice Periodical on Structural Design and Construction*, 13(4), 2008, pp. 175-185.
27. De Luca, A. and Guidi, L.G., State of Art in the Worldwide Evolution of Base Isolation Design, *Soil Dynamics and Earthquake Engineering*, 125, 2019, Article 105722.
28. Sheikh, H., Van Engelen, N.C., and Ruparathna, R., A Review of Base Isolation Systems with Adaptive Characteristics, *Structures*, 38, 2022, pp. 1542-1555.
29. Santoso, A. K., Sulistyo, D., Awaludin, A., Setiawan, A. F., Satyarno, I., Purnomo, S., and Harry, I., Structural systems Comparison of Simply Supported PSC Box Girder Bridge Equipped with Elastomeric Rubber Bearing and Lead Rubber Bearing, *Civil Engineering Dimension*, 24(1), 2022, pp. 19-30.
30. Wang, X. and Hutchinson, T.C., Elastic and Inelastic Acceleration Amplification of Nonstructural Components Characterized using Recorded Building Responses, *Engineering Structures*, 302, 2024, Article 117306.
31. Cardone, D., Flora, A., and Gesualdi, G., Inelastic Response of RC Frame Buildings with Seismic Isolation, *Earthquake Engineering & Structural Dynamics*, 42(6), 2013, pp. 871-889.
32. Lu, X., Wang, D., and Wang, S., Investigation of the Seismic Response of High-rise Buildings Supported on Tension-resistant Elastomeric Isolation Bearings, *Earthquake Engineering & Structural Dynamics*, 45(13), 2016, pp. 2207-2228.
33. Anajafi, H., Poursadr, K., Roohi, M., and Santini-Bell, E., Effectiveness of Seismic Isolation for Long-period Structures Subject to Far-field and Near-field Excitations, *Frontiers in Built Environment*, 6, 2020, Article 24.
34. Jangid, R.S., Optimum Lead-rubber Isolation Bearings for Near-fault Motions, *Engineering Structures*, 29(10), 2007, pp. 2503-2513.
35. Hu, J.W., Response of Seismically Isolated Steel Frame Buildings with Sustainable Lead-rubber Bearing (LRB) Isolator Devices Subjected to Near-fault (NF) Ground Motions, *Sustainability*, 7(1), 2014, pp. 111-137.
36. Shoaei, P., Orimi, H.T., and Zahrai, S.M., Seismic Reliability-based Design of Inelastic Base-isolated Structures with Lead-rubber Bearing Systems, *Soil Dynamics and Earthquake Engineering*, 115, 2018, pp. 589-605.
37. Kim, J.H., Kim, M.K., and Choi, I.K., Experimental Study on Seismic Behavior of Lead-rubber Bearing Considering Bi-directional Horizontal Input Motions, *Engineering Structures*, 198, 2019, Article 109529.

38. Yurdakul, M. and Yıldız, M.B., A Study on Seismic Isolation of Building Used LRB, *Challenge Journal of Structural Mechanics*, 6(2)**,** 2020, pp. 52-60.
39. Raheem, S.A., Omar, M., Zaher, A.A., and Taha, A., Effects of Numerical Modeling Simplification on Seismic Design of Buildings, *Coupled Systems Mechanics*, 7(6)**,** 2018a, pp. 731-753.
40. Raheem, S.A., Zaher, A.A., and Taha, A., Finite Element Modeling Assumptions Impact on Seismic Response Demands of MRF-buildings, *Earthquake Engineering and Engineering Vibration*, 17**,** 2018b, pp. 821-834.
41. Chandra, J., Lokito, V. N., and Tambuna, J. A., Seismic Performance of Precast Concrete Special Moment Frames with Hybrid Connection System in Five and Ten Story Buildings, *Civil Engineering Dimension*, 25(2), 2023, pp. 85-95.
42. Ma, X.T., Bao, C., Doh, S.I., Lu, H., Zhang, L.X., Ma, Z.W., and He, Y.T., Dynamic Response Analysis of Story-adding Structure with Isolation Technique Subjected to Near-fault Pulse-like Ground Motions, *Physics and Chemistry of the Earth*, 121**,** 2021, Article 102957.
43. Liu, L., Liu, D., Zhang, L., Li, Q., Ma, B., Shan, H., and Lei, M., Study on Seismic Response of Staggered Story Isolated Structure Under Ordinary and Long-period Earthquake, *Journal of Vibration Engineering & Technologies*, 12(1)**,** 2024, pp. 667-679.
44. Zhao, T., Liu, D., Guo, Z., Shan, H., Huo, Y., Li, X., and Lei, M., Study on the Overturning Resistance of a New Staggered Story Isolated Structure, *Structures*, 65**,** 2024, Article 106709.
45. Zhou, W., Huang, C., Li, X., Liu, D., Zhang, Y., and Fang, S., Analysis of Shock Absorption Performance of a New Staggered Story Isolation Structure Under Far-field Long-period Ground Motions, *Soil Dynamics and Earthquake Engineering*, 177**,** 2024, Article 108411.
46. Shu, T., Li, H., Wang, T., Liu, D., Yao, S., and Lei, M., Study on the Seismic Response of New Staggered Story Isolated Structure Under Different Parameters, *Frontiers in Earth Science*, 11, 2023, Article 1115235.
47. Chimamphant, S. and Kasai, K., Comparative Response and Performance of Base-isolated and Fixed-base Structures, *Earthquake Engineering & Structural Dynamics*, 45(1)**,** 2016, pp. 5-27.
48. Mazza, F., Seismic Demand of Base-isolated Irregular Structures Subjected to Pulse-type Earthquakes, *Soil Dynamics and Earthquake Engineering*, 108**,** 2018, pp. 111-129.
49. Mazza, F., Mazza, M., and Vulcano, A., Base-isolation Systems for the Seismic Retrofitting of RC Framed Buildings with Soft-storey Subjected to Near-fault Earthquakes, *Soil Dynamics and Earthquake Engineering*, 109**,** 2018, pp. 209-221.
50. Mazza, F., Effects of the Long-term Behaviour of Isolation Devices on the Seismic Response of Base-isolated Buildings, *Structural Control and Health Monitoring*, 26(4)**,** 2019, Article e2331.
51. Deringöl, A.H. and Güneyisi, E.M., Single and Combined Use of Friction-damped and Base-isolated Systems in Ordinary Buildings, *Journal of Constructional Steel Research*, 174**,** 2020, Article 106308.
52. Zelleke, D.H. and Matsagar, V.A., Multi-hazard Stochastic Response Assessment of Base-isolated Buildings, *Structure and Infrastructure Engineering*, 20(3)**,** 2024, pp. 301-325.
53. Bhandari, M., Bharti, S.D., Shrimali, M.K., and Datta, T.K., The Numerical Study of Base-isolated Buildings Under Near-field and Far-field Earthquakes, *Journal of Earthquake Engineering*, 22(6)**,** 2018, pp. 989-1007.
54. Shahbazi, S., Mansouri, I., Hu, J.W., and Karami, A., Effect of Soil Classification on Seismic Behavior of SMFs Considering Soil-Structure Interaction and Near-field Earthquakes, *Shock and Vibration*, 2018(1)**,** 2018, Article 4193469.
55. IS 1893 (Part 1), *Criteria for Earthquake Resistant Design of Structures*, Bureau of Indian Standards, New Delhi, 2016.
56. IS 1893 (Part 6), *Base Isolated Buildings - Criteria for Earthquake Resistant Design of Structures*, Bureau of Indian Standards, New Delhi, 2022.
57. IS 875 (Part 1), *Code of Practice for Design Loads (Other than Earthquake) for Buildings and Structures – Dead Loads: Unit Weights of Building Materials and Stored Materials*, Bureau of Indian Standards, New Delhi, 1987.
58. IS 875 (Part 2), *Code of Practice for Design Loads (Other than Earthquake) for Buildings and Structures – Imposed Loads*, Bureau of Indian Standards, New Delhi, 1987.
59. IS 875 (Part 5), *Code of Practice for Design Loads (Other than Earthquake) for Buildings and Structures – Special Loads and Load Combinations*, Bureau of Indian Standards, New Delhi, 1987.
60. Shirol, S. and Kori, J.J., Seismic Base Isolation of RC Frame Structures with and without Infill, *International Research Journal of Engineering and Technology*, 4**,** 2017, pp. 1783-1792.

APPENDIX

A G+7 storey building model was created on plain ground, and the maximum reaction was determined for the specified load combination in IS 875 Part 1, Part 2, and Part 5. Based on this maximum reaction and the target bearing time period, an LRB was designed. Figure 18 illustrates the maximum support reaction for the selected load combination.

Generally, isolation bearings are designed for 2.5 to 3.5 times the vibration period of the building, as per IS 1893 (Part 6): 2022. In this study, the bearing is designed for 3 times the period of building. Targeted designed effective natural period of LRB (T_{eff}).

1. Maximum reaction (W) = 3622 kN (obtained from the analysis, as shown in Figure 19)
2. The vibration period of the building (T) = 1.25 s
3. $T_{eff} = 3*T = 3.75$ s (as per IS 1893 (Part 6): 2022)
4. $K_{eff} = \left(\frac{2\pi}{T_{eff}}\right)^2 \frac{W}{g} = 1036$ kN/m
5. As per IS 1893 (part 6): 2022 Clause 6.1,
   Displacement at isolator level (S_D) = $\beta \left[z\frac{Sa}{g}\right] g * \left(\frac{T\_eff}{2\pi}\right)^2$
   Zone factor Z = 0.36, $\frac{Sa}{g} = \frac{1}{T_{eff}}$ as per IS 1893 (part1) :2016, and β = 0.8165.
   Thus, S_D= 0.273 m.
6. Energy dissipated in single cycle = $2\pi K_{eff} (S_D)^2 \beta = 48.55$ kNm
7. Assuming, $\frac{Q_d}{W}$ =0.06
   $Q_d = 0.06*3622 = 217$ kN
8. Diameter of the lead (D_L) = $\sqrt{\frac{4Qd}{\pi\sigma_l}} = 0.166$m
9. Outer diameter of the LRB (D_2) = 4* D_L = 0.664 and area of bearing (A_b) = 0.325m^2
10. Shape factor (S) = $(D_2^2 - D_L^2/(4D_2t_r)$
    Assuming t_r in the range of 3mm to 15 mm, taking it as 10mm and no. of layers = 25
    Therefore, the total thickness of bearing (T_r) = 25*10 = 250mm
    The thickness of each steel shim = 3mm
    Total height of bearing (H) = 10*25+(25-1) *3+2*50 = 422mm = 0.422m
    Hence, S = 15.6
11. Post yield Stiffness (K_d) = $K_{eff} - Q_d/S_D$
    $K_d = 1036 - 217/0.273 = 240$ kN/m

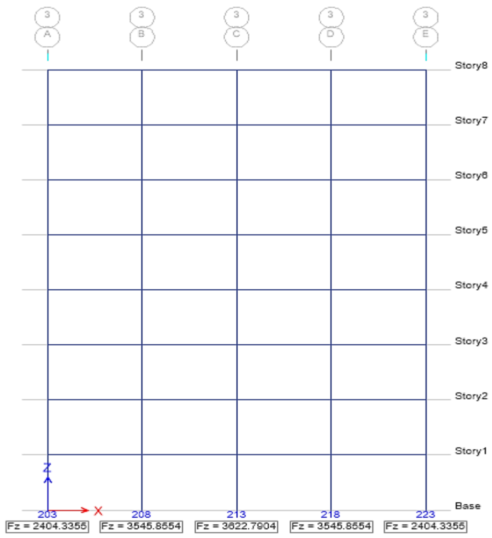

Figure 18. Maximum Support Reactions

12. Post to pre-yield stiffness ratio (α) = 0.1
13. Elastic stiffness (k_{el}) = $K_d/0.1 = 240/0.1 = 2400$ kN/m
14. Yield force = $Q_d/ (1- \alpha) = 241$ kN
15. Yield Displacement (y) = $F_y/K_{el} = 0.1249$m
16. Axial vertical stiffness (K_v) = $A*E_c/T_r$
17. $Ec = \left[\frac{1}{6GS^2} + \frac{4}{3K}\right]^{-1}$
    Where G is the Modulus of Rigidity assumed 1 MPa (in the range of 0.6 to 1.2 Mpa) and K is the bulk modulus

of 2000 MPa.
Therefore, E_c = 7399906 kN/m^3

18. K_v = 961872 kN/m.

From the above investigation, the obtained parameters are summarized in Table 3.